Journal of Applied Analysis and Computation
Volume 13, Number 4, August 2023, 2203–2228
Website:http://www.jaac-online.com
DOI:10.11948/20220446

AN EFFICIENT PARAMETER UNIFORM SPLINE-BASED TECHNIQUE FOR SINGULARLY PERTURBED WEAKLY COUPLED REACTION-DIFFUSION SYSTEMS

Satpal Singh[1,†], Devendra Kumar[1] and Higinio Ramos[2,3]

Abstract A parameter-uniform numerical scheme for a system of weakly coupled singularly perturbed reaction-diffusion equations of arbitrary size with appropriate boundary conditions is investigated. More precisely, quadratic B-spline basis functions with an exponentially graded mesh are used to solve a $\ell \times \ell$ system whose solution exhibits parabolic (or exponential) boundary layers at both endpoints of the domain. A suitable mesh-generating function is used to generate the exponentially graded mesh. The decomposition of the solution into regular and singular components is obtained to provide error estimates. A convergence analysis is addressed, which shows a uniform convergence of the second order. To validate the theoretical findings, two test problems are solved numerically.

Keywords Singularly perturbed system, reaction-diffusion equations, parameter-uniform convergence, exponentially graded mesh, boundary layers.

MSC(2010) 65L10, 65L11, 65L60, 65M50.

1. Introduction

In many areas of science and engineering, we often face problems whose solution has a multi-scale behavior, *i.e.,* in some parts of the domain, the solution changes very rapidly, and in other parts, it changes slowly. These problems are referred to as singularly perturbed problems (SPPs). The regions where the solution changes rapidly are referred to as the layer regions, and the parts of the domain where the solution changes slowly are referred to as the outer regions (or regular regions). These problems are frequent in many branches of science and engineering, such as fluid dynamics, quantum mechanics, chemical reactor theory, elasticity, and porous gas electrode theory. These problems contain small parameters multiplying the higher-order derivative terms. The coefficient ε of the highest order derivative term characterizes the diffusion coefficient, and the order of the differential equation

[†]The corresponding author.
Email: satpalsingh1704@gmail.com(S. Singh),
dkumar@pilani.bits-pilani.ac.in(D. Kumar), higra@usal.es(H. Ramos)
[1]Department of Mathematics, Birla Institute of Technology and Science, Pilani, Rajasthan-333031, India
[2]Scientific Computing Group, Universidad de Salamanca, Plaza de la Merced, 37008 Salamanca, Spain
[3]Escuela Politécnica Superior de Zamora, Campus Viriato, 49029 Zamora, Spain

reduces when ε is set to zero. In the layer region, the solution's derivatives are significantly larger than those in the regular part, so classical numerical methods fail to solve these problems, and unacceptably large oscillations occur in these regions (see [13, 38, 45] for reference). To overcome this difficulty, one has to use a non-conventional scheme. In particular, there are two popular strategies for dealing with these problems. The first one is the use of fitted-operator methods that reflect the nature of the solution in the boundary layers and can be implemented on an equidistant mesh, while the second one is the use of layer-adapted meshes. Although fitted operator methods use a uniform mesh, they are easy to implement, and their convergence analysis is more straightforward compared to methods based on non-uniform meshes. These methods have a major drawback; one can not construct an ε-uniform fitted operator method on an equidistant mesh when there are parabolic boundary layers in the solution (see Chapter 11 of [38] for completion). Another area for improvement with this approach is the difficulty of extending these methods to multidimensional problems in complex domains. Additionally, fitted mesh methods require knowing the location and thickness of the boundary layers to generate highly appropriate non-uniform grids. For several non-uniform grids such as Shishkin, Bakhvalov, or Bakhvalov-Shishkin (B-S) meshes, the readers are referred to [16, 17, 23, 24, 27, 41]. This phenomenon determines the evolution of parameter-uniform numerical methods *i.e.,* the methods in which the error constant is independent of ε and the mesh parameter.

Various ε-uniform numerical schemes such as the variational method, the finite difference methods (FDMs), the rational spectral collocation methods, the finite element methods (FEMs), the adaptive mesh methods, and the layer-adapted mesh methods have been developed for singularly perturbed boundary value problems (SPBVPs) (readers are referred to [1, 11–13, 18–20, 32] and the references therein). Although the Shishkin mesh is one of the simplest non-uniform meshes; it has a drawback, that is before one attempts to solve the differential equation, significant information about the exact solution must be known. Often this information is not available, especially for nonlinear problems. Thus, a different approach can be used, namely the use of an adaptive non-uniform grid where the adaptivity is governed by the numerical solution. This approach does not require a priori information about the solution of the problem. Due to this advantage, these grids (referred to as solution-adaptive grids) have become extremely popular and have been successfully used in widespread applications. In this paper, we construct an adaptive grid, namely exponentially graded mesh, sufficient to settle the issue of the boundary layers.

Starting in the late 1960s, in this evolution process, several numerical methods (independent of ε) have been constructed for a scalar reaction-diffusion equation (see, [2, 38, 43, 45] and the references therein). On the other hand, less effort has been devoted to systems of reaction-diffusion boundary value problems. For a system of two coupled singularly perturbed reaction-diffusion equations, with diffusion coefficients $\varepsilon_1, \varepsilon_2$, depending on the relation and values of ε_1 and ε_2 three cases are of interest (i) $\varepsilon_1, \varepsilon_2$ arbitrary, (ii) $\varepsilon_1 = \varepsilon, \varepsilon_2 = 1$, and (iii) $\varepsilon_1 = \varepsilon_2 = \varepsilon$ (see [47]). Some schemes and their corresponding convergence analyses for these particular cases can be seen in [31, 34, 35], where a parameter-uniform convergence of the first order was established. We cite some works about systems of SPBVPs: Matthews *et al.* [36] proposed classical finite difference operators with special piecewise-uniform meshes to solve a system of two coupled reaction-diffusion equations. Madden and

Stynes [32] suggested the first-order parameter-uniform central difference scheme with a variant of Shishkin mesh for a coupled system of two singularly perturbed linear reaction-diffusion equations. Using the basic ideas of the perturbation method, Valanarasu and Ramanujam [53] suggested exponentially fitted FDMs to solve a class of weakly coupled systems of singularly perturbed reaction-diffusion equations. For a coupled system of equations containing different magnitudes diffusion parameters Linß and Madden [25] considered a central difference scheme on layer-adapted piecewise uniform meshes. They established that their scheme is almost second-order parameter-uniform convergent, which is an improvement on the scheme proposed in [32]. Linß and Madden [26] suggested a FEM on general layer-adapted meshes (Shishkin and Bakhvalov meshes) for a system of two coupled reaction-diffusion equations. They have shown that the method is of first-order and almost first-order (up to a logarithmic factor) parameter-uniform convergent with Bakhvalov and Shishkin meshes, respectively. Natesan and Deb [40] devised a second-order uniformly convergent hybrid scheme for a singularly perturbed system of reaction-diffusion equations. The scheme comprises a cubic spline scheme in the layer region and the classical central difference scheme elsewhere. Clavero *et al.* [5] presented a non-monotone FDM of HODIE type on a Shishkin mesh for the coupled systems of singularly perturbed reaction-diffusion equations. They have shown that the scheme is a parameter-uniform convergent of orders two and three in the cases of different and equal diffusion parameters, respectively. They have also addressed a hybrid FDM of HODIE type on a piecewise uniform Shishkin mesh for the coupled systems of singularly perturbed reaction-diffusion equations [6]. They have shown that the discretized operator satisfies the discrete maximum principle, and the scheme is almost a third-order parameter-uniform convergent (except for a logarithmic factor).

Das and Natesan [9] proposed a second-order central difference scheme with the adaptively generated graded mesh for a system of coupled singularly perturbed reaction-diffusion equations. In the system, they have taken diffusion parameters with different magnitudes. Lin and Stynes [22] considered a FEM for a system of coupled reaction-diffusion equations, where each equation has the same diffusion coefficient. The method was used with a Shishkin mesh and showed an almost first-order convergent, independent of the magnitude of the diffusion parameter. Constructing an adaptive layer mesh using the equidistribution principle for a positive monitor function, Das and Aguiar [10] proposed an accurate second-order scheme for a system of reaction-diffusion equations. Singh and Natesan [49] applied the nonsymmetric discontinuous Galerkin FEM with interior penalties on a piecewise-uniform Shishkin mesh to obtain the numerical solution of a system of reaction-diffusion equations. They have shown that the method is k-th order uniformly convergent in the energy norm, where k is the polynomial degree. In some of the above articles, the equations have diffusion parameters of different magnitudes, while diffusion parameters of the same magnitudes were taken in some works.

Motivation: These systems of equations frequently arise in several applications in science and engineering, as in electroanalytical chemistry [47], predator-prey population dynamics [15], the turbulent interaction of waves and currents [44,52], chemical reactor theory [46], the classical linear double-diffusion model for saturated flow in fractured porous media [3], modelling of the diffusion process in bones [8], and control theory [39]. Only a few articles have appeared dealing with systems of arbitrary size; to cite a few, Linß and Madden [28] proposed a parameter-uniform central difference scheme on layer-adapted meshes (Shishkin, Bakhvalov, and Equidistribution meshes). They have shown that the method is second-order accurate on the Bakhvalov and Equidistribution meshes, while it is almost second-order accurate up to a logarithmic factor on a Shishkin mesh. Linß suggested a FEM on arbitrary meshes (layer-adapted meshes) for a system of $\ell \geqslant 2$ singularly perturbed reaction-diffusion equations. Theoretically, he has shown that the error bounds for the Shishkin meshes are lower than those on the Bakhvalov meshes. Stephens and Madden [51] developed the discrete Schwarz method on three overlapping subdomains for an arbitrarily sized coupled singularly perturbed systems. They have used standard FDM on a uniform mesh on each subdomain and proved that the method is parameter-uniform when appropriate subdomains are used. In this paper, we consider a $\ell \times \ell$ system of singularly perturbed reaction-diffusion equations in which the equations have diffusion parameters of the same magnitudes. We use an exponentially graded mesh for the discretization which results in a second-order (without logarithmic factor) parameter-uniform convergence. The proposed scheme extends the method developed for a single singularly perturbed reaction-diffusion BVP [30] to a system of reaction-diffusion equations.

We propose and analyze a parameter-uniform numerical method that uses quadratic B-spline basis functions with a special non-uniform exponentially graded mesh [7, 48, 50, 55]. In [7], Constantinou and Xenophontos analyzed h version FEM in the natural energy norm for the singularly perturbed class of reaction-diffusion and convection-diffusion problems. Shivhare *et al.* [48] constructed a quadratic B-spline-based parameter uniform numerical scheme of second order in space and first order in time for two parameter singularly perturbed PDEs. Exploring the degenerate parabolic problems, Singh *et al.* [50] proposed a uniformly convergent method and proved second-order convergence on the exponentially graded mesh. Zarin [55] developed the h-version of the standard Galerkin method using higher order polynomials and proved its robust convergence in the energy norm.

We consider the following singularly perturbed problem, which involves a system of ℓ weakly coupled reaction-diffusion equations. We seek a solution $\boldsymbol{u} \in (C^2(0,1) \cap C[0,1])^\ell$ that satisfies

$$\boldsymbol{\mathcal{L}}\boldsymbol{u}(x) := -\boldsymbol{\mathcal{E}}\boldsymbol{u}''(x) + \boldsymbol{B}(x)\boldsymbol{u}(x) = \boldsymbol{g}(x),\ x \in (0,1), \tag{1.1a}$$

subject to the Dirichlet boundary conditions

$$\boldsymbol{u}(0) = \boldsymbol{\varrho}_0,\ \boldsymbol{u}(1) = \boldsymbol{\varrho}_1, \tag{1.1b}$$

where $\boldsymbol{\mathcal{L}} = (\mathcal{L}_1, \dots, \mathcal{L}_\ell)^T$, $\boldsymbol{\mathcal{E}} = \operatorname{diag}(\varepsilon_1^2, \varepsilon_2^2, \dots, \varepsilon_\ell^2)$ with $\varepsilon_k = \varepsilon,\ k = 1, 2, \dots, \ell$, $\boldsymbol{B}(x) = (b_{ij}(x))_{\ell\times\ell}$, $\boldsymbol{g}(x) = (g_1(x), g_2(x), \dots, g_\ell(x))^T$, $\boldsymbol{u}(x) = (u_1(x), u_2(x), \dots, u_\ell(x))^T$, $\boldsymbol{\varrho}_0 = (\varrho_{0,1}, \dots, \varrho_{0,\ell})^T$, and $\boldsymbol{\varrho}_1 = (\varrho_{1,1}, \dots, \varrho_{1,\ell})^T$. We assume that each column of the coupling matrix $\boldsymbol{B} : [0,1] \to \mathbb{R}^{(\ell,\ell)}$ and the function $\boldsymbol{g} : [0,1] \to \mathbb{R}^\ell$ belong to $C^4[0,1]^\ell$. We assume that the following inequality holds to fulfill the condition of the strongly diagonally dominant matrix along with the nonsingularity of $\boldsymbol{B}(x)$ $\forall x \in [0,1]$

$$\sum_{\substack{k=1 \\ k\neq i}}^{\ell} \left\| \frac{b_{ik}}{b_{ii}} \right\| < 1, \text{ for } i = 1, 2, \dots, \ell. \tag{1.2}$$

The paper is organized as follows: Section 2 gives some preliminary results on the solution and its derivatives. A decomposition of the exact solution is also provided in this section. The scheme is proposed in Section 3, divided into two subsections: in subsection 3.1, an exponentially graded mesh is constructed, and the collocation scheme is given in subsection 3.2. The comprehensive convergence analysis is provided in Section 4. Numerical simulations and discussion of the results are exemplified in Section 5, while some concluding comments and further research in this direction are included in Section 6.

Throughout the paper, matrices and vectors will be denoted by bold letters, while we use plain letters for scalars. A superscript T will be used to transpose a vector/matrix. When the domain $\mathcal{D}$ is obvious, the standard notation $\|.\|$ will be used (instead of $\|.\|_{\mathcal{D}}$) for the infinity-norm ($L^{\infty}-$norm) e.g., for a scalar function U defined on an interval I, we define $\|U\| = \max_{x\in I}|U(x)|$ while for a vector valued function $\boldsymbol{U} = (U_1, U_2, \ldots, U_\ell)^T \in \mathbb{R}^\ell$, defined on I, the infinity-norm is defined as $\|\boldsymbol{U}\| = \max_{x\in I}\{|U_1(x)|, |U_2(x)|, \ldots, |U_\ell(x)|\}$. For simplicity, for any function U, we use U_j for $U(x_j)$ and $\widetilde{U}_j$ for an approximation of U at x_j. For a vector valued function $\boldsymbol{U} = (U_1, U_2, \ldots, U_\ell)^T \in \mathbb{R}^\ell$ applied to x_j we use the notation $(U_1, U_2, \ldots, U_\ell)^T(x_j) = (U_{1,j}, U_{2,j}, \ldots, U_{\ell,j})^T$. Furthermore, $\boldsymbol{C} = (C, C, \ldots, C)^T$ denotes a generic positive constant vector independent of the perturbation parameter ε, the nodal points x_j, and the mesh parameter N_x. A subscripted C (e.g., C_1) is also a constant independent of ε, x_j, and N_x, but whose value is fixed. Furthermore, we use $C^0(\mathcal{D})$ for the set of continuous functions in $\mathcal{D}$, and $C^k(\mathcal{D})$ for k times continuously differentiable functions in $\mathcal{D}$. Moreover, $C^k(\mathcal{D})^\ell$ is used for k times continuously differentiable vector-valued functions (with ℓ components) in $\mathcal{D}$.

2. Preliminary: Properties of the exact solution

In this section, we show some bounds on the solution $\boldsymbol{u}$ and its derivatives which will be used in the convergence analysis.

Theorem 2.1. *Assume that $\boldsymbol{B}$ satisfies the following conditions to be a strongly diagonally dominant matrix*

$$b_{ii} > 0, \;\; \textit{and} \; \sum_{\substack{k=1\\k\neq i}}^{\ell}\left\|\frac{b_{ik}}{b_{ii}}\right\| < \xi < 1, \;\; \xi \in (0,1), \;\; \textit{for}\; i = 1, 2, \ldots, \ell.$$

Then

$$|u_i^{(k)}(x)| \leqslant C\left\{1 + \varepsilon^{-k}\left(e^{-\lambda x/\varepsilon} + e^{-\lambda(1-x)/\varepsilon}\right)\right\}, \;\; \textit{for}\; k = 0, 1, 2; \;\; i = 1, 2, \ldots, \ell,$$

where $\lambda = \lambda(\xi) > 0$ is given by

$$\lambda^2 = (1-\xi) \min_{i=1,2,\ldots,\ell}\left\{\min_{x\in[0,1]} b_{ii}(x)\right\}.$$

Proof. Refer to the proof of Theorem 2.4 given in [28]. □

In the study of numerical simulation of SPBVPs, stability estimates ensure the boundedness of the solution. Note that we assumed that the coupling matrix $\boldsymbol{B}$ is an arbitrary matrix with positive diagonal entries. We give the following stability criterion using the maximum principle (refer to Protter and Weinberger [42]).

Lemma 2.1 (Stability Estimate)**.** *Consider the differential operator*

$$\widetilde{\mathcal{L}}u := -\nu^2 u'' + c(x)u' + b(x)u,$$

with $\nu > 0$, $b, c \in C[0,1]$ *and* $b(x) > 0$ *on* $[0,1]$. *Then*

$$\|\mathcal{V}\| \leqslant \max\left\{ \left\| \frac{\widetilde{\mathcal{L}}\mathcal{V}}{b} \right\|, |\mathcal{V}(0)|, |\mathcal{V}(1)| \right\}, \text{ for all } \mathcal{V} \in C^2(0,1) \cap C[0,1].$$

We decompose the solution of problem (1.1) as $\boldsymbol{u} = \boldsymbol{\varphi} + \boldsymbol{\eta}$, with $\boldsymbol{\varphi} = (\varphi_1, \ldots, \varphi_\ell)^T$, and $\boldsymbol{\eta} = (\eta_1, \ldots, \eta_\ell)^T$, where the components satisfy the following BVPs, respectively

$$-\varepsilon^2 \varphi_i''(x) + b_{ii}(x)\varphi_i(x) = g_i(x),\ x \in (0,1),\ \varphi_i(0) = \varrho_{0,i},\ \varphi_i(1) = \varrho_{1,i},\ i = 1, 2, \ldots, \ell,$$

and

$$-\varepsilon^2 \eta_i''(x) + b_{ii}(x)\eta_i(x) = -\sum_{\substack{k=1\\k\neq i}}^{\ell} b_{ik}(x)u_k(x),\ x \in (0,1),\ \eta_i(0) = \eta_i(1) = 0,\ i = 1, 2, \ldots, \ell.$$

Using Lemma 2.1, we obtain

$$\|\varphi_i\| \leqslant \max\left\{ \left\| \frac{g_i}{b_{ii}} \right\|, |\varrho_{0,i}|, |\varrho_{1,i}| \right\}, \text{ and } \|\eta_i\| \leqslant \sum_{\substack{k=1\\k\neq i}}^{\ell} \left\| \frac{b_{ik}}{b_{ii}} \right\| \|u_k\| \text{ for } i = 1, 2, \ldots, \ell.$$

Now, since $\|u_i\| \leqslant \|\varphi_i\| + \|\eta_i\|$, we have

$$\|u_i\| - \sum_{\substack{k=1\\k\neq i}}^{\ell} \left\| \frac{b_{ik}}{b_{ii}} \right\| \|u_k\| \leqslant \max\left\{ \left\| \frac{g_i}{b_{ii}} \right\|, |\varrho_{0,i}|, |\varrho_{1,i}| \right\} \text{ for } i = 1, 2, \ldots, \ell.$$

We consider the matrix

$$\boldsymbol{G} = \begin{bmatrix} 1 & -\|b_{12}/b_{11}\| & \ldots & -\|b_{1\ell}/b_{11}\| \\ -\|b_{21}/b_{22}\| & 1 & \ldots & -\|b_{2\ell}/b_{22}\| \\ \vdots & \vdots & \ddots & \vdots \\ -\|b_{\ell 1}/b_{\ell\ell}\| & -\|b_{\ell 2}/b_{\ell\ell}\| & \ldots & 1 \end{bmatrix}, \tag{2.1}$$

such that all entries of $\boldsymbol{G}^{-1}$ are non-negative, then u is bounded for the given data.

Theorem 2.2. *Assuming that the coupling matrix* $\boldsymbol{B}$ *has positive diagonal entries, the matrix* $\boldsymbol{G}$ *is inverse monotone. Then the solution* $\boldsymbol{u}$ *of (1.1) satisfies*

$$\|u_i\| \leqslant \sum_{k=1}^{\ell} (\boldsymbol{G}^{-1})_{ik} \max\left\{ \left\| \frac{g_i}{b_{ii}} \right\|, |\varrho_{0,i}|, |\varrho_{1,i}| \right\}, \text{ for } i = 1, 2, \ldots, \ell.$$

Proof. The condition (1.2) implies that the matrix $\boldsymbol{G}$ is a strictly diagonally dominant L_0-matrix, and the inverse monotonicity of $\boldsymbol{G}$ is directed by the M-matrix criterion. The proof follows using Lemma 2.1 (see [27–29] for the details). □

Remark 2.1. In general, the operator $\boldsymbol{\mathcal{L}}$ does not satisfy the maximum principle, but Theorem 2.2 suggests that $\boldsymbol{\mathcal{L}}$ is stable in the maximum-norm sense.

Remark 2.2. The existence and uniqueness of the solution $\boldsymbol{u} \in C^4[0,1]^\ell$ is guaranteed by the following arguments:
(a) The stability estimates of the vector-differential operator $\boldsymbol{\mathcal{L}}$ using the standard arguments given in [21] (b) The coupling matrix $\boldsymbol{B}$ and the vector-valued function $\boldsymbol{g}$ belong to the space of twice continuously differentiable functions.

Due to the presence of boundary layers, we need to examine the solution in regular and layer regions. So, we decompose $\boldsymbol{u}$ into three parts as follows:

$$\boldsymbol{u} = \boldsymbol{v} + \boldsymbol{w}_L + \boldsymbol{w}_R,$$

where $\boldsymbol{v}$ is the regular component, $\boldsymbol{w}_L$ and $\boldsymbol{w}_R$ are termed as the left and right singular components, respectively. These components are the solutions of the following BVPs, respectively:

$$-\boldsymbol{\mathcal{E}}\boldsymbol{v}''(x) + \boldsymbol{B}(x)\boldsymbol{v}(x) = \boldsymbol{g}(x),\ x \in (0,1),\ \boldsymbol{v}(0) = \boldsymbol{B}(0)^{-1}\boldsymbol{g}(0),\ \boldsymbol{v}(1) = \boldsymbol{B}(1)^{-1}\boldsymbol{g}(1), \tag{2.2a}$$

$$-\boldsymbol{\mathcal{E}}\boldsymbol{w}_L''(x) + \boldsymbol{B}(x)\boldsymbol{w}_L(x) = 0,\ x \in (0,1),\ \boldsymbol{w}_L(0) = \boldsymbol{\varrho}_0 - \boldsymbol{v}(0),\ \boldsymbol{w}_L(1) = 0, \tag{2.2b}$$

and

$$-\boldsymbol{\mathcal{E}}\boldsymbol{w}_R''(x) + \boldsymbol{B}(x)\boldsymbol{w}_R(x) = 0,\ x \in (0,1),\ \boldsymbol{w}_R(0) = 0,\ \boldsymbol{w}_R(1) = \boldsymbol{\varrho}_1 - \boldsymbol{v}(1). \tag{2.2c}$$

Theorem 2.3. *The components $\boldsymbol{v}$, $\boldsymbol{w}_L$, and $\boldsymbol{w}_R$ satisfy*

$$|v_i^{(k)}| \leqslant C, \quad \textit{for } k = 0,1,\ldots,4;\ i = 1,2,\ldots,\ell, \tag{2.3a}$$

$$|(w_L)_i^{(k)}| \leqslant C\varepsilon^{-k}e^{-\lambda x/\varepsilon}, \quad \textit{for } k = 0,1,\ldots,4;\ i = 1,2,\ldots,\ell, \tag{2.3b}$$

$$|(w_R)_i^{(k)}| \leqslant C\varepsilon^{-k}e^{-\lambda(1-x)/\varepsilon}, \quad \textit{for } k = 0,1,\ldots,4;\ i = 1,2,\ldots,\ell. \tag{2.3c}$$

Proof. An explanatory proof is given in [6]. □

3. The proposed scheme

In this section, first, we give the detail of the construction of the non-uniform mesh. Then, we introduce and implement the proposed scheme for problem (1.1).

3.1. Mesh construction

It is well-known that standard numerical schemes on an equidistant mesh fail to solve SPBVPs and unexpectedly large oscillations appear near the layer region(s) when we use a classical numerical technique. In other words, we can generate a scheme on an equidistant mesh that converges at all mesh points uniformly in the diffusion parameter unless an unacceptably large number of mesh points are used. It is not practical at all; thus, to resolve the layer(s), a non-uniform mesh is required. In this section, we construct an exponentially graded mesh that generates more mesh points in the layer region than in the other part of the domain.

To construct the exponentially graded mesh $\Delta = \{x_j|\ 0 \leqslant j \leqslant N_x\}$, we split the interval $[0,1]$ into $N_x > 4$ (with N_x a multiple of 4) subintervals $I_j = [x_{j-1}, x_j]$.

We denote by $\mathcal{P}_p$, the space of all polynomials of degree $\leqslant p$. In the construction of the mesh, we require a mesh generating function $\Psi(\rho)$, which belongs to a class of piecewise continuously differentiable functions, monotonically increasing in nature, and defined as

$$\Psi(\rho) = -\ln(1 - 2\mathfrak{C}_{p,\varepsilon}\rho), \;\; \rho \in [0, 1/2 - 1/N_x], \tag{3.1}$$

where $\mathfrak{C}_{p,\varepsilon} = 1 - \exp\left(-\frac{1}{(p+1)\varepsilon}\right) \in \mathbb{R}^+$. With the help of the transition points $x_{\frac{N_x}{4}-1}$ and $x_{\frac{3N_x}{4}+1}$, we split the interval $[0,1]$ into three subintervals such that $[0,1] = [0, x_{\frac{N_x}{4}-1}] \cup [x_{\frac{N_x}{4}-1}, x_{\frac{3N_x}{4}+1}] \cup [x_{\frac{3N_x}{4}+1}, 1]$. The nodal points can be written in the following form

$$x_j = \begin{cases} (p+1)\varepsilon\Psi(\rho_j), \quad j = 0, 1, \ldots, \dfrac{N_x}{4} - 1, \\[2ex] x_{\frac{N_x}{4}-1} + \left(\dfrac{x_{\frac{3N_x}{4}+1} - x_{\frac{N_x}{4}-1}}{\frac{N_x}{2} + 2}\right)(j - N_x/4 + 1), \quad j = \dfrac{N_x}{4}, \ldots, \dfrac{3N_x}{4}, \\[2ex] 1 - (p+1)\varepsilon\Psi(1 - \rho_j), \quad j = \dfrac{3N_x}{4} + 1, \ldots, N_x, \end{cases}$$

where $\rho_j = \frac{j}{N_x}$ for $j = 0, 1, \ldots, N_x$, and $\widetilde{h}_j = x_j - x_{j-1}$ for $j = 1, 2, \ldots, N_x$. The mesh points are distributed equidistantly in $[x_{\frac{N_x}{4}-1}, x_{\frac{3N_x}{4}+1}]$ with $N_x/2 + 2$ subintervals, and exponentially graded in $[0, x_{\frac{N_x}{4}-1}]$ and $[x_{\frac{3N_x}{4}+1}, 1]$ with $N_x/4 - 1$ subintervals in each. The mesh step lengths $\widetilde{h}_j$ satisfy the following inequalities utilizing the mesh characterizing function $\Phi = \exp(-\Psi)$ (see [7] for more details)

$$\widetilde{h}_j \leqslant \begin{cases} C(p+1)\varepsilon N_x^{-1} \max \Psi'(\rho_j) \leqslant C(p+1)\varepsilon N_x^{-1} \max |\Phi^{'}(\rho_j)| \exp\left(\dfrac{x_j}{(p+1)\varepsilon}\right), \\[2ex] j = 1, 2, \ldots, \dfrac{N_x}{4} - 1, \\[2ex] CN_x^{-1}, \quad j = \dfrac{N_x}{4}, \ldots, \dfrac{3N_x}{4} + 1, \\[2ex] C(p+1)\varepsilon N_x^{-1} \max \Psi'(1-\rho_j) \leqslant C(p+1)\varepsilon N_x^{-1} \max |\Phi^{'}(1-\rho_j)| \exp\left(\dfrac{1-x_j}{(p+1)\varepsilon}\right), \\[2ex] j = \dfrac{3N_x}{4} + 2, \ldots, N_x. \end{cases}$$

Since $\max |\Phi^{'}| < 2$, we can simply write the above inequalities as

$$\widetilde{h}_j \leqslant \begin{cases} C\varepsilon N_x^{-1} \exp\left(\dfrac{x_j}{(p+1)\varepsilon}\right), \quad j = 1, 2, \ldots, \dfrac{N_x}{4} - 1, \\[2ex] CN_x^{-1}, \quad j = \dfrac{N_x}{4}, \ldots, \dfrac{3N_x}{4} + 1, \\[2ex] C\varepsilon N_x^{-1} \exp\left(\dfrac{1 - x_j}{(p+1)\varepsilon}\right), \quad j = \dfrac{3N_x}{4} + 2, \ldots, N_x, \end{cases} \tag{3.2}$$

and the step lengths of this adaptive mesh satisfy the following estimates

$$|\widetilde{h}_{j+1}-\widetilde{h}_j| \leqslant C \begin{cases} \varepsilon N_x^{-2}, & j=1,2,\ldots,\dfrac{N_x}{4}-1,\\ 0, & j=\dfrac{N_x}{4},\ldots,\dfrac{3N_x}{4},\\ \varepsilon N_x^{-2}, & j=\dfrac{3N_x}{4}+1,\ldots,N_x. \end{cases} \tag{3.3}$$

Remark 3.1. Near the transition points, the Shishkin and Bakhvalov meshes do not satisfy the inequality $|\tilde{h}_{i+1}-\tilde{h}_i| \leq CN_x^{-2}$. Thus, we cannot extend our analysis to these meshes.

3.2. Discretization of the problem

In this section, considering the collocation approach, we discretize problem (1.1) using piecewise quadratic C^1-splines. We denote the mesh intervals by $I_j=[x_{j-1},x_j]$, and the collocation points are chosen as midpoints of these intervals *i.e.,*

$$X_j = x_{j-1/2} := \frac{x_{j-1}+x_j}{2} = x_{j-1}+\frac{\widetilde{h}_j}{2} = x_j-\frac{\widetilde{h}_j}{2}, \quad \text{for } j=1,2,\ldots,N_x.$$

For $m,p\in\mathbb{N}\,(m<p)$, we define

$$S_p^m(\Delta) := \{r\in C^m[0,1]:\ r|_{I_j}\in\mathcal{P}_p,\ \text{for } j=1,2,\ldots,N_x\}.$$

To discretize (1.1), we consider a vector of splines whose components are in $S_2^1(\Delta)$ and satisfies the BVP (1.1) at certain points. It is known that the midpoints of $I_j,\ j=1,2,\ldots,N_x$, are the best choice for collocation with quadratic C^1-splines for regularly perturbed BVPs (see [4]). Next, we define the quadratic nonuniform and nonsmooth splines $\mathfrak{B}_j(x)\in S_2^1(\Delta)$ for $j=0,1,2,\ldots,N_x,N_x+1$ as follows:

$$\mathfrak{B}_0(x)=\begin{cases} \dfrac{(x_1-x)^2}{\widetilde{h}_1^2}, & x_0\leqslant x\leqslant x_1,\\ 0, & \text{otherwise}, \end{cases}$$

$$\mathfrak{B}_1(x)=\begin{cases} \dfrac{\widetilde{h}_1^2-(x_1-x)^2}{\widetilde{h}_1^2}+\dfrac{(x-x_0)^2}{\widetilde{h}_1(\widetilde{h}_1+\widetilde{h}_2)}, & x_0\leqslant x\leqslant x_1,\\ \dfrac{(x_2-x)^2}{\widetilde{h}_1(\widetilde{h}_1+\widetilde{h}_2)}, & x_1\leqslant x\leqslant x_2,\\ 0, & \text{otherwise}, \end{cases}$$

and for $j=2,3,\ldots,N_x-1$,

$$\mathfrak{B}_j(x)=\begin{cases} \dfrac{(x-x_{j-2})^2}{\widetilde{h}_{j-1}(\widetilde{h}_{j-1}+\widetilde{h}_j)}, & x_{j-2}\leqslant x\leqslant x_{j-1},\\ \dfrac{(x-x_{j-2})(x_j-x)}{\widetilde{h}_j(\widetilde{h}_{j-1}+\widetilde{h}_j)}+\dfrac{(x_{j+1}-x)(x-x_{j-1})}{\widetilde{h}_j(\widetilde{h}_j+\widetilde{h}_{j+1})}, & x_{j-1}\leqslant x\leqslant x_j,\\ \dfrac{(x_{j+1}-x)^2}{\widetilde{h}_{j+1}(\widetilde{h}_j+\widetilde{h}_{j+1})}, & x_j\leqslant x\leqslant x_{j+1},\\ 0, & \text{otherwise}, \end{cases}$$

while for $j = N_x,\ N_x+1$ these are given as

$$\mathfrak{B}_{N_x}(x) = \begin{cases} \dfrac{(x-x_{N_x-2})^2}{\widetilde{h}_{N_x-1}(\widetilde{h}_{N_x-1}+\widetilde{h}_{N_x})}, & x_{N_x-2} \leqslant x \leqslant x_{N_x-1}, \\ \dfrac{\widetilde{h}_{N_x}^2-(x-x_{N_x-1})^2}{\widetilde{h}_{N_x}^2} + \dfrac{(x_{N_x}-x)^2}{\widetilde{h}_{N_x}(\widetilde{h}_{N_x-1}+\widetilde{h}_{N_x})}, & x_{N_x-1} \leqslant x \leqslant x_{N_x}, \\ 0, \quad \text{otherwise}, \end{cases}$$

$$\mathfrak{B}_{N_x+1}(x) = \begin{cases} \dfrac{(x-x_{N_x-1})^2}{\widetilde{h}_{N_x}^2}, & x_{N_x-1} \leqslant x \leqslant x_{N_x}, \\ 0, \quad \text{otherwise}. \end{cases}$$

The discretization consists of finding $\tilde{\boldsymbol{u}}$ whose components are in $S_2^1(\Delta)$ such that

$$\tilde{\boldsymbol{u}}_0 = \tilde{\boldsymbol{u}}(0) = \boldsymbol{\varrho}_0,\ (\boldsymbol{\mathcal{L}}\tilde{\boldsymbol{u}})_{j-1/2} = \boldsymbol{g}_{j-1/2},\ \tilde{\boldsymbol{u}}_{N_x} = \tilde{\boldsymbol{u}}(1) = \boldsymbol{\varrho}_1,\ j = 1,2,\dots,N_x. \tag{3.4}$$

Using the component-wise form (for $k = 1,2,\dots,\ell$), it can be written as

$$(\tilde{u}_k)_0 = \varrho_{0,k},\ (\mathcal{L}_k\tilde{u}_k)_{j-1/2} = (g_k)_{j-1/2},\ (\tilde{u}_k)_{N_x} = \varrho_{1,k},\ j = 1,2,\dots,N_x. \tag{3.5}$$

We represent each component of the collocation solution $\tilde{\boldsymbol{u}}$ as

$$\tilde{u}_k(x) = \sum_{j=0}^{N_x+1} \alpha_{j,k}\mathfrak{B}_j(x), \quad k = 1,2,\dots,\ell, \tag{3.6}$$

where the coefficients $\alpha_{j,k}$ can be determined by solving the following system obtained by using (3.6) in (3.4). This system can be written in the form

$$\alpha_{0,k} = \varrho_{0,k},\ [\boldsymbol{L\alpha}_k]_{j-1/2} = \boldsymbol{g}_{j-1/2},\ j = 1,2,\dots,N_x,\ \alpha_{N_x+1,k} = \varrho_{1,k},\ k = 1,2,\dots,\ell, \tag{3.7}$$

where $[\boldsymbol{L\alpha}_k]_{j-1/2}$ comes from the discretization of $(\boldsymbol{\mathcal{L}}\tilde{\boldsymbol{u}})_{j-1/2}$ and is given by

$$\begin{aligned} [\boldsymbol{L\alpha}_k]_{j-1/2} :=& -\varepsilon^2\left[\frac{2(\alpha_{j+1,k}-\alpha_{j,k})}{\widetilde{h}_j(\widetilde{h}_j+\widetilde{h}_{j+1})} - \frac{2(\alpha_{j,k}-\alpha_{j-1,k})}{\widetilde{h}_j(\widetilde{h}_j+\widetilde{h}_{j-1})}\right] \\ &+ \sum_{m=1}^{\ell}(b_{km})_{j-1/2}\left[q_j^+\alpha_{j+1,k} + \left(1-q_j^+-q_j^-\right)\alpha_{j,k} + q_j^-\alpha_{j-1,k}\right], \\ &j = 1,2,\dots,N_x, \end{aligned}$$

where $q_j^+ := \frac{\widetilde{h}_j}{4(\widetilde{h}_j+\widetilde{h}_{j+1})}$ and $q_j^- := \frac{\widetilde{h}_j}{4(\widetilde{h}_j+\widetilde{h}_{j-1})}$. Combining all the equations, we get the system

$$\boldsymbol{A\wp} = \mathfrak{G},$$

where

$$\begin{aligned} \mathfrak{G} = \Big(&\underbrace{\varrho_{0,1}, g_1(X_1),\dots,g_1(X_{N_x}),\varrho_{1,1}}_{1^{\text{st}}\text{component}}, \underbrace{\varrho_{0,2}, g_2(X_1),\dots,g_2(X_{N_x}),\varrho_{1,2}}_{2^{\text{nd}}\text{component}},\dots\dots, \\ &\underbrace{\varrho_{0,\ell}, g_\ell(X_1),\dots,g_\ell(X_{N_x}),\varrho_{1,\ell}}_{\ell^{\text{th}}\text{component}}\Big)^T, \end{aligned}$$

$$\boldsymbol{\wp} = \Bigg(\underbrace{\alpha_{0,1}, \alpha_{1,1}, \ldots, \alpha_{N_x,1}, \alpha_{N_x+1,1}}_{1^{\text{st}}\text{component}}, \underbrace{\alpha_{0,2}, \alpha_{1,2}, \ldots, \alpha_{N_x,2}, \alpha_{N_x+1,2}}_{2^{\text{nd}}\text{component}}, \ldots,$$
$$\underbrace{\alpha_{0,\ell}, \alpha_{1,\ell}, \ldots, \alpha_{N_x,\ell}, \alpha_{N_x+1,\ell}}_{\ell^{\text{th}}\text{component}}\Bigg)^T.$$

The matrix $\boldsymbol{A}$ is given as

$$\boldsymbol{A} = \begin{bmatrix} A_{11} & A_{12} & \ldots & A_{1\ell} \\ A_{21} & A_{22} & \ldots & A_{2\ell} \\ \vdots & \vdots & \ddots & \vdots \\ A_{\ell 1} & A_{\ell 2} & \ldots & A_{\ell\ell} \end{bmatrix},$$

where each A_{km} is a submatrix of order $(N_x+2) \times (N_x+2)$. These submatrices are given by

$$A_{kk} = \begin{bmatrix} 1 & 0 & 0 & 0 & \ldots & \ldots & 0 \\ a_{21,kk} & a_{22,kk} & a_{23,kk} & 0 & \ldots & \ldots & 0 \\ 0 & a_{32,kk} & a_{33,kk} & a_{34,kk} & \ldots & \ldots & 0 \\ \vdots & \ddots & \ddots & \ddots & \vdots & \vdots & \vdots \\ \ldots & \ldots & \ldots & 0 & a_{N_x+1N_x,kk} & a_{N_x+1N_x+1,kk} & a_{N_x+1N_x+2,kk} \\ \ldots & \ldots & \ldots & 0 & 0 & 0 & 1 \end{bmatrix},$$

where

$$\begin{aligned} a_{ii-1,kk} &= -\frac{8\varepsilon^2 q_{i-1}^-}{\widetilde{h}_{i-1}^2} + b_{kk}(X_{i-1})q_{i-1}^-, \\ a_{ii,kk} &= \frac{8\varepsilon^2 q_{i-1}^+}{\widetilde{h}_{i-1}^2} - \frac{8\varepsilon^2 q_{i-1}^-}{\widetilde{h}_{i-1}^2} + b_{kk}(X_{i-1})\Big(1 - q_{i-1}^+ - q_{i-1}^-\Big), \\ a_{ii+1,kk} &= -\frac{8\varepsilon^2 q_{i-1}^+}{\widetilde{h}_{i-1}^2} + b_{kk}(X_{i-1})q_{i-1}^+, \end{aligned}$$

for $i = 2, 3, \ldots, N_x + 1$. Furthermore, for $m \neq k,\ m = 1, 2, \ldots, \ell;\ k = 1, 2, \ldots, \ell$, the submatrix A_{km} is

$$A_{km} = \begin{bmatrix} 0 & 0 & 0 & 0 & \ldots & \ldots & 0 \\ a_{21,km} & a_{22,km} & a_{23,km} & 0 & \ldots & \ldots & 0 \\ 0 & a_{32,km} & a_{33,km} & a_{34,km} & \ldots & \ldots & 0 \\ \vdots & \ddots & \ddots & \ddots & \vdots & \vdots & \vdots \\ \ldots & \ldots & \ldots & 0 & a_{N_x+1N_x,km} & a_{N_x+1N_x+1,km} & a_{N_x+1N_x+2,km} \\ \ldots & \ldots & \ldots & 0 & 0 & 0 & 0 \end{bmatrix},$$

where

$$\begin{aligned} a_{ii-1,km} &= b_{km}(X_{i-1})q_{i-1}^{-}, \\ a_{ii,km} &= b_{km}(X_{i-1})\left(1 - q_{i-1}^{+} - q_{i-1}^{-}\right), \\ a_{ii+1,km} &= b_{km}(X_{i-1})q_{i-1}^{+}, \end{aligned}$$

for $i = 2, 3, \ldots, N_x + 1$.

4. Convergence Analysis

4.1. S_2^0-interpolation

To find the interpolation $I_2^0\boldsymbol{y}$ whose components are in $S_2^0(\Delta)$, we solve the following interpolation problem assuming that $y_k \in C^0[0,1]$:

$$(I_2^0 y_k)_j = (y_k)_j,\ j = 0, 1, \ldots, N_x, \quad \text{and} \quad (I_2^0 y_k)_{j-1/2} = (y_k)_{j-1/2},\ j = 1, 2, \ldots, N_x,$$

where $(y_k)_j = y_k(x_j),\ (y_k)_{j-1/2} = y_k(X_j),\ k = 1, 2, \ldots, \ell.$

Theorem 4.1. *Assuming $b_{ij}(x), g_j(x) \in C^4[0,1]$, for $i,\ j = 1, 2, \ldots, \ell$, the interpolation error $\boldsymbol{u} - I_2^0\boldsymbol{u}$ of the solution $\boldsymbol{u}$ of (1.1) satisfies the following bounds:*

$$\|\boldsymbol{u} - I_2^0\boldsymbol{u}\| \leqslant CN_x^{-3}, \quad \textit{and} \quad \boldsymbol{\mathcal{E}} \max_{j=1,2,\ldots,N_x} |(\boldsymbol{u} - I_2^0\boldsymbol{u})''_{j-1/2}| \leqslant \boldsymbol{C}N_x^{-2}.$$

Proof. First, we make use of the Lagrange representation of the interpolation polynomial and Taylor expansions to verify that for any $\boldsymbol{y} \in C^4[0,1]^\ell$, the interpolation error on each I_j satisfies

$$\left\|y_k - I_2^0 y_k\right\|_{I_j} \leqslant \frac{\widetilde{h}_j^3}{24}\left\|y_k^{(3)}\right\|_{I_j}, \quad \left|(y_k - I_2^0 y_k)''_{j-1/2}\right| \leqslant \frac{\widetilde{h}_j^2}{48}\left\|y_k^{(4)}\right\|_{I_j}, \ k = 1, 2, \ldots, \ell. \quad (4.1)$$

Using the linear property of I_2^0, the solution components u_k can be decomposed as

$$u_k - I_2^0 u_k = (v_k - I_2^0 v_k) + \left((w_L)_k - I_2^0(w_L)_k\right) + \left((w_R)_k - I_2^0(w_R)_k\right).$$

We start this analysis by finding the interpolation error in the regular component. For $I_j \subset [x_0, x_{N_x/4-1}]$, we use the bounds given in Theorem 2.3, to obtain

$$\begin{aligned} \frac{\widetilde{h}_j^3}{24}\left|v_k^{(3)}\right|_{I_j} &\leqslant C\varepsilon^3 N_x^{-3} \exp\left(\frac{3x_j}{(p+1)\varepsilon}\right) \\ &\leqslant CN_x^{-3} \exp\left(\frac{x_j}{\varepsilon}\right) \\ &\leqslant CN_x^{-3} \exp\Big((p+1)\Psi(\rho_j)\Big) \\ &\leqslant CN_x^{-3}. \end{aligned}$$

Similarly, using the same analysis in the right layer region $I_j \subset [x_{3N_x/4+2}, x_{N_x}]$, we obtain $\|v_k - I_2^0 v_k\|_{I_j} \leqslant CN_x^{-3}$. Also, for $I_j \subset [x_{N_x/4}, x_{3N_x/4+1}]$, the bounds for $\widetilde{h}_j$

(using Equation (3.2)) trivially give $\|v_k - I_2^0 v_k\|_{I_j} \leqslant CN_x^{-3}$. Thus, by combining all the estimates for the regular component, we get

$$\|v_k - I_2^0 v_k\| \leqslant CN_x^{-3}.$$

Next, we consider the left singular component $(w_L)_k$ in $I_j \subset [x_0, x_{N_x/4-1}]$. Using Theorem 2.3 and the inequality given in (3.2), we get

$$\begin{aligned}
\frac{\widetilde{h}_j^3}{24}\left|(w_L)_k^{(3)}\right|_{I_j} &\leqslant C\varepsilon^3 N_x^{-3} \exp\left(\frac{3x_j}{(p+1)\varepsilon}\right)\varepsilon^{-3}|e^{-\lambda x/\varepsilon}|_{I_j} \\
&\leqslant CN_x^{-3} \exp\left(\frac{x_j}{\varepsilon} - \frac{x_{j-1}}{\varepsilon}\right) \\
&\leqslant CN_x^{-3} \exp\left(\frac{\widetilde{h}_j}{\varepsilon}\right) \\
&\leqslant CN_x^{-3} \exp\left((p+1)N_x^{-1} \max \Psi'(\rho_j)\right) \\
&\leqslant CN_x^{-3}.
\end{aligned}$$

Now for $I_j \subset [x_{N_x/4}, x_{3N_x/4+1}]$, we obtain

$$\begin{aligned}
\frac{\widetilde{h}_j^3}{24}\left|(w_L)_k^{(3)}\right|_{I_j} &\leqslant CN_x^{-3}\varepsilon^{-3}|e^{-\lambda x/\varepsilon}|_{I_j} \\
&\leqslant CN_x^{-3}\varepsilon^{-3} \exp\left(-\frac{\lambda x_{j-1}}{\varepsilon}\right).
\end{aligned}$$

Using L'Hôpital's rule, it is easy to see that the term $\varepsilon^{-3}\exp\left(-\frac{\lambda x_{j-1}}{\varepsilon}\right)$ is bounded in $[x_{N_x/4}, x_{3N_x/4+1}]$. Thus, the above inequality gives

$$\frac{\widetilde{h}_j^3}{24}\left|(w_L)_k^{(3)}\right|_{I_j} \leqslant CN_x^{-3}.$$

Similar bounds can be obtained for $I_j \subset [x_{3N_x/4+2}, x_{N_x}]$ using the same arguments as for $[x_0, x_{N_x/4-1}]$. Thus, we get

$$\|(w_L)_k - I_2^0 (w_L)_k\| \leqslant CN_x^{-3}.$$

Now for the right singular component $(w_R)_k$ in $I_j \subset [x_0, x_{N_x/4-1}]$ (using Theorem 2.3 and the inequality in (3.2)), we get

$$\begin{aligned}
\frac{\widetilde{h}_j^3}{24}\left|(w_R)_k^{(3)}\right|_{I_j} &\leqslant C\varepsilon^3 N_x^{-3} \exp\left(\frac{3x_j}{(p+1)\varepsilon}\right)\varepsilon^{-3}|e^{-\lambda(1-x)/\varepsilon}|_{I_j} \\
&\leqslant C\varepsilon^3 N_x^{-3} \exp\left(\frac{C_1 x_j}{\varepsilon}\right)\varepsilon^{-3} \exp\left(-\frac{C_2(1-x_{j-1})}{\varepsilon}\right) \\
&\leqslant CN_x^{-3} \exp\left(C_3 \frac{x_j - (1-x_{j-1})}{\varepsilon}\right) \\
&\leqslant CN_x^{-3} \exp\left(C_3 \frac{\widetilde{h}_j - 1 - 2x_{j-1}}{\varepsilon}\right)
\end{aligned}$$

$$\leqslant CN_x^{-3}\exp\Big(C_3(p+1)N_x^{-1}\max\Psi'(\rho_j)\Big)$$
$$\leqslant CN_x^{-3}.$$

Following the same approach as we have done for $(w_L)_k$ in the intervals $[x_{N_x/4}, x_{3N_x/4+1}]$ and $[x_{3N_x/4+2}, x_{N_x}]$, we obtain

$$\|(w_R)_k - I_2^0(w_R)_k\| \leqslant CN_x^{-3}.$$

Next, we find the bounds for $\max\limits_{j=1,2,\ldots,N_x} |(u_k - I_2^0 u_k)''_{j-1/2}|$. For this purpose, first, we consider v_k in $I_j \subset [x_0, x_{N_x/4-1}]$ as follows

$$\begin{aligned}\frac{\widetilde{h}_j^2}{48}\Big|v_k^{(4)}\Big|_{I_j} &\leqslant C\varepsilon^2 N_x^{-2}\exp\Big(\frac{2x_j}{(p+1)\varepsilon}\Big)\text{(using Theorem 2.3 and the inequality in (3.2))}\\ &\leqslant CN_x^{-2}\exp\Big(\frac{2x_j}{(p+1)\varepsilon}\Big)\\ &\leqslant CN_x^{-2}\exp\Big(2\Psi(\rho_j)\Big)\\ &\leqslant CN_x^{-2}.\end{aligned}$$

Similar results can be obtained for the intervals $[x_{N_x/4}, x_{3N_x/4+1}]$ and $[x_{3N_x/4+2}, x_{N_x}]$. Now for the left singular component in $I_j \subset [x_0, x_{N_x/4-1}]$, we have

$$\begin{aligned}\frac{\widetilde{h}_j^2}{48}\Big|(w_L)_k^{(4)}\Big|_{I_j} &\leqslant C\varepsilon^2 N_x^{-2}\exp\Big(\frac{2x_j}{(p+1)\varepsilon}\Big)\varepsilon^{-4}|e^{-\lambda x/\varepsilon}|_{I_j}\\ &\leqslant C\varepsilon^2 N_x^{-2}\exp\Big(\frac{C_1 x_j}{\varepsilon}\Big)\varepsilon^{-4}\exp\Big(\frac{-C_2 x_{j-1}}{\varepsilon}\Big)\\ &\leqslant C\varepsilon^{-2}N_x^{-2}\exp\Big(\frac{C_3(x_j - x_{j-1})}{\varepsilon}\Big)\\ &\leqslant C\varepsilon^{-2}N_x^{-2}\exp\Big(\frac{C_3\widetilde{h}_j}{\varepsilon}\Big)\\ &\leqslant C\varepsilon^{-2}N_x^{-2}\exp\Big(C_3(p+1)N_x^{-1}\max\Psi'(\rho_j)\Big)\\ &\leqslant C\varepsilon^{-2}N_x^{-2}.\end{aligned}$$

A similar procedure can obtain the same bounds for the intervals $[x_{N_x/4}, x_{3N_x/4+1}]$ and $[x_{3N_x/4+2}, x_{N_x}]$. Thus, we have

$$\max_{j=1,2,\ldots,N_x} |((w_L)_k - I_2^0(w_L)_k)''_{j-1/2}| \leqslant C\varepsilon^{-2}N_x^{-2}.$$

Furthermore, one can use a similar analogy to find the bounds for the right singular component $(w_R)_k$. Finally, using the triangle inequality leads us to complete the proof. □

Lemma 4.1. *Let $s_k \in S_2^0(\Delta)$ with $(s_k)_{j-1/2} = 0,\ j = 1, 2, \ldots, N_x;\ k = 1, 2, \ldots, \ell$, then*

$$\|s_k\|_{I_j} \leqslant \max_j\{|(s_k)_{j-1}|, |(s_k)_j|\}, \quad \|s_k''\|_{I_j} \leqslant \frac{8}{\widetilde{h}_j^2}\max_j\{|(s_k)_{j-1}|, |(s_k)_j|\}.$$

Proof. Refer to [48] for a complete proof. □

4.2. S_2^1-interpolation

To find the interpolation $I_2^1 y_k \in S_2^1(\Delta)$ assuming that $y_k \in C^1[0,1]$, we solve the following interpolation problem:

$$(I_2^1 y_k)_0 = (y_k)_0, \quad (I_2^1 y_k)_{j-1/2} = (y_k)_{j-1/2},\ j = 1,2,\dots,N_x, \quad (I_2^1 y_k)_{N_x} = (y_k)_{N_x}, \tag{4.2}$$

where $(y_k)_{j-1/2} = y_k(X_j),$ for $k = 1,2,\dots,\ell$.

Let $\Lambda : S_2^1(\Delta) \to \mathbb{R}^{N_x+1}$ be the operator defined by

$$[\Lambda s_k]_j = a_j(s_k)_{j-1} + 3(s_k)_j + c_j(s_k)_{j+1},$$

where $a_j = \frac{\widetilde{h}_{j+1}}{\widetilde{h}_j+\widetilde{h}_{j+1}}$ and $c_j = 1 - a_j = \frac{\widetilde{h}_j}{\widetilde{h}_j+\widetilde{h}_{j+1}}$. Then from [14,33], we have

$$\begin{aligned}[\Lambda s_k]_j &\equiv a_j(s_k)_{j-1} + 3(s_k)_j + c_j(s_k)_{j+1} \\ &= 4a_j(s_k)_{j-1/2} + 4c_j(s_k)_{j+1/2},\ j = 1,2,\dots,N_x-1.\end{aligned} \tag{4.3}$$

Lemma 4.2. *The operator Λ in (4.3) is stable, with $(s_k)_0 = (s_k)_{N_x} = 0$,*

$$\max_{j=1,2,\dots,N_x-1} |(s_k)_j| \leqslant \frac{1}{2}\left\{\max_{j=1,2,\dots,N_x-1} |[\Lambda s_k]_j|\right\}, \quad k = 1,2,\dots,\ell,$$

for $s_k \in \mathbb{R}^{N_x+1}$.

Proof. Refer to Lemma 3 given in [30]. □

Theorem 4.2. *Assume that $b_{ij}(x), g_j(x) \in C^4[0,1]$, for $i, j = 1,2,\dots,\ell$, then the interpolation error $\boldsymbol{u} - I_2^1\boldsymbol{u}$ of the solution $\boldsymbol{u}$ of (1.1) satisfies the following bounds*

$$\max_{j=0,1,\dots,N_x} |(\boldsymbol{u} - I_2^1\boldsymbol{u})_j| \leqslant \boldsymbol{C}N_x^{-4}, \tag{4.4a}$$

$$\|\boldsymbol{u} - I_2^1\boldsymbol{u}\| \leqslant CN_x^{-3}, \tag{4.4b}$$

$$\boldsymbol{\mathcal{E}} \max_{j=1,2,\dots,N_x} |(\boldsymbol{u} - I_2^1\boldsymbol{u})''_{j-1/2}| \leqslant \boldsymbol{C}N_x^{-2}. \tag{4.4c}$$

Proof. For the interpolation error $y_k - I_2^1 y_k$, we consider an arbitrary function y_k that satisfies

$$(y_k - I_2^1 y_k)_0 = (y_k - I_2^1 y_k)_{N_x} = 0, \quad k = 1,2,\dots,\ell.$$

Using the definitions of S_2^1-interpolation and the operator Λ given by (4.2) and (4.3), respectively, we have

$$\tau_{y_k,j} = [\Lambda(y_k - I_2^1 y_k)]_j = a_j(y_k)_{j-1} - 4a_j(y_k)_{j-1/2} + 3(y_k)_j - 4c_j(y_k)_{j+1/2} + c_j(y_k)_{j+1}, \tag{4.5}$$

for $j = 1,2,\dots,N_x,$ $k = 1,2,\dots,\ell$. Furthermore, we use the Taylor series expansions to get

$$|\tau_{y_k,j}| \leqslant \frac{1}{12}\widetilde{h}_j\widetilde{h}_{j+1}|\widetilde{h}_{j+1} - \widetilde{h}_j||(y_k''')_j|_{I_j} + \frac{5}{96}\max\{\widetilde{h}_j^4, \widetilde{h}_{j+1}^4\}\|(y_k^{(4)})_j\|_{I_j\cup I_{j+1}}. \tag{4.6}$$

Now, the interpolation error can be decomposed as

$$u_k - I_2^1 u_k = (v_k - I_2^1 v_k) + \Big((w_L)_k - I_2^1(w_L)_k\Big) + \Big((w_R)_k - I_2^1(w_R)_k\Big),$$

or

$$\tau_{u_k,j} = \tau_{v_k,j} + \tau_{(w_L)_k,j} + \tau_{(w_R)_k,j}.$$

To find the error, we start considering the regular component. For $I_j \subset [x_0, x_{N_x/4-1}]$, we use Theorem 2.3 and the inequality (4.6), to get

$$|\tau_{v_k,j}| \leqslant C\Big(\widetilde{h}_j\widetilde{h}_{j+1}|\widetilde{h}_{j+1} - \widetilde{h}_j| + \max\{\widetilde{h}_j^4, \widetilde{h}_{j+1}^4\}\Big).$$

Now as $\widetilde{h}_j < \widetilde{h}_{j+1}$ holds in $[x_0, x_{N_x/4-1}]$, so

$$\begin{aligned}
|\tau_{v_k,j}| &\leqslant C\Big(\widetilde{h}_{j+1}^2|\widetilde{h}_{j+1} - \widetilde{h}_j| + \widetilde{h}_{j+1}^4\Big)\\
&\leqslant C\bigg(\varepsilon^3 N_x^{-4}\exp\bigg(\frac{2x_{j+1}}{(p+1)\varepsilon}\bigg) + \varepsilon^4 N_x^{-4}\exp\bigg(\frac{4x_{j+1}}{(p+1)\varepsilon}\bigg)\bigg)\\
&\leqslant CN_x^{-4}\exp\bigg(\frac{4x_{j+1}}{(p+1)\varepsilon}\bigg)\\
&\leqslant CN_x^{-4}\exp\Big(4\Psi(\rho_{j+1})\Big)\\
&\leqslant CN_x^{-4}.
\end{aligned}$$

Moreover, for $x_j \in [x_{N_x/4}, x_{3N_x/4+1}]$, it is obvious to prove that $|\tau_{v_k,j}| \leqslant CN_x^{-4}$. A similar bound can be proved for $x_j \in [x_{3N_x/4+2}, x_{N_x}]$. Therefore, using Lemma 4.2, we get

$$\max_{j=0,1,\ldots,N_x} |(v_k - I_2^1 v_k)_j| \leqslant CN_x^{-4}.$$

Now in the process of finding the bounds for $(w_L)_k$, we use the fact that $\widetilde{h}_j < \widetilde{h}_{j+1}$ for $x_j \in [x_0, x_{N_x/4-1}]$, which yields

$$\begin{aligned}
|\tau_{(w_L)_k,j}| &\leqslant \frac{1}{12}\widetilde{h}_j\widetilde{h}_{j+1}|\widetilde{h}_{j+1} - \widetilde{h}_j||(w_L''')_{k,j}|_{I_j} + \frac{5}{96}\max\{\widetilde{h}_j^4, \widetilde{h}_{j+1}^4\}\|(w_L^{(4)})_{k,j}\|_{I_j\cup I_{j+1}}\\
&\leqslant C\Big(\widetilde{h}_{j+1}^2|\widetilde{h}_{j+1} - \widetilde{h}_j|\varepsilon^{-3}|e^{-\lambda x/\varepsilon}|_{I_j} + \widetilde{h}_{j+1}^4\varepsilon^{-4}|e^{-\lambda x/\varepsilon}|_{I_j\cup I_{j+1}}\Big)\\
&\leqslant C\bigg(N_x^{-4}\exp\bigg(\frac{2x_{j+1}}{(p+1)\varepsilon}\bigg)|e^{-\lambda x/\varepsilon}|_{I_j} + N_x^{-4}\exp\bigg(\frac{4x_{j+1}}{(p+1)\varepsilon}\bigg)|e^{-\lambda x/\varepsilon}|_{I_j\cup I_{j+1}}\bigg)\\
&\leqslant CN_x^{-4}\exp\bigg(\frac{C_1\widetilde{h}_{j+1}}{\varepsilon}\bigg)\\
&\leqslant CN_x^{-4}\exp\Big(C_1(p+1)N_x^{-1}\max\Psi'(\rho_{j+1})\Big)\\
&\leqslant CN_x^{-4}.
\end{aligned}$$

Similar bounds can be obtained in $[x_{3N_x/4+2}, x_{N_x}]$. Moreover, it is easy to prove $\tau_{(w_L)_k,j} \leqslant CN_x^{-4}$ for $x_j \in [x_{N_x/4}, x_{3N_x/4+1}]$. Therefore, using Lemma 4.2, we get

$$\max_{j=0,1,\ldots,N_x} |((w_L)_k - I_2^1(w_L)_k)_j| \leqslant CN_x^{-4}.$$

Similar arguments can be used to derive the bounds for the right singular component $(w_R)_k$ (we skip the analysis here). The estimate given in (4.4a) can be attained directly by combining all the interpolation errors for three components. To prove (4.4b), we use the triangle inequality as

$$\begin{aligned}\|\boldsymbol{u}-I_2^1\boldsymbol{u}\| &\leqslant \|\boldsymbol{u}-I_2^0\boldsymbol{u}\|+\|I_2^0\boldsymbol{u}-I_2^1\boldsymbol{u}\| \\ &\leqslant \|\boldsymbol{u}-I_2^0\boldsymbol{u}\|+\max_{j=0,1,\dots,N_x}|(\boldsymbol{u}-I_2^1\boldsymbol{u})_j|.\end{aligned}$$

Now using the fact $(I_2^1\boldsymbol{u})_j=\boldsymbol{u}_j,\ j=0,1,\dots,N_x$, Lemma 4.1, Theorem 4.1, and (4.4a), we obtain the estimate (4.4b). Furthermore, to obtain the inequality (4.4c), we use the same approach as we have used for (4.4b). For this purpose, we write

$$\begin{aligned}|(u_k-I_2^1u_k)''_{j-1/2}| &\leqslant |(u_k-I_2^0u_k)''_{j-1/2}|+|(I_2^0u_k-I_2^1u_k)''_{j-1/2}| \\ &\leqslant |(u_k-I_2^0u_k)''_{j-1/2}|+\max_{j=0,1,\dots,N_x}\frac{8}{\widetilde{h}_j^2}|(u_k-I_2^1u_k)_j|.\end{aligned}$$

Hence, the proof is completed using Theorem 4.1 and inequality (4.4a). □

Theorem 4.3. *We assume that there exists a constant* $\mu>0$ *such that*

$$\max\{\widetilde{h}_{j+1},\widetilde{h}_{j-1}\}\geqslant\mu\widetilde{h}_j,\quad j=1,2,\dots,N_x-1,\ \widetilde{h}_1\geqslant\mu\widetilde{h}_2,\ \text{and}\ \widetilde{h}_{N_x}\geqslant\mu\widetilde{h}_{N_x-1}.$$

Then the operator L_k *is stable in the maximum-norm being*

$$\begin{aligned}&\|\boldsymbol{\gamma}_k\|\leqslant 3\max_{j=1,2,\dots,N_x}\left|\frac{[L_k\boldsymbol{\gamma}_k]_{j-1/2}}{n_{j-1/2,k}}\right|,\quad k=1,2,\dots,\ell,\\ &\text{for all } \boldsymbol{\gamma}_k\in\mathbb{R}_0^{N_x+2}=\{r\in\mathbb{R}^{N_x+2}: r_0=r_{N_x+1}=0\},\end{aligned}$$

where $n_{j-1/2,k}:=\displaystyle\sum_{m=1}^{\ell}(b_{km})_{j-1/2}\left(1-q_j^+-q_j^-\right),\ j=1,2,\dots,N_x,\ k=1,2,\dots,\ell.$

Proof. Note that $q_j^+,\ q_j^-\in(0,1/4)$, therefore $n_{j,k}>0,\ j=1,2,\dots,N_x$. For arbitrary vectors $\boldsymbol{\gamma}_k\in\mathbb{R}_0^{N_x+2}$, we define the operators $\boldsymbol{\Lambda}_k$ by

$$[\boldsymbol{\Lambda}_k\boldsymbol{\gamma}_k]_{j-1/2}=-\frac{\varepsilon^2}{n_{j-1/2,k}}\left[\frac{2(\gamma_{j+1,k}-\gamma_{j,k})}{\widetilde{h}_j(\widetilde{h}_j+\widetilde{h}_{j+1})}-\frac{2(\gamma_{j,k}-\gamma_{j-1,k})}{\widetilde{h}_j(\widetilde{h}_j+\widetilde{h}_{j-1})}\right]+\gamma_{j,k},\ j=1,2,\dots,N_x.$$

The operators $\boldsymbol{\Lambda}_k$ are well defined due to the positivity of all $n_{j-1/2,k}$. Proceeding as in [30], we get the required result. □

Theorem 4.4. *Let* $\boldsymbol{u}$ *be the exact solution to (1.1) and* $\tilde{\boldsymbol{u}}$ *is its approximation on the exponentially graded mesh, then*

$$\|\boldsymbol{u}-\tilde{\boldsymbol{u}}\|\leqslant CN_x^{-2}.$$

Proof. We generalize the approach given in [50] for a scalar problem to a system. Using the triangle inequality, we have

$$\|u_k-\tilde{u}_k\|\leqslant\|u_k-I_2^1u_k\|+\|I_2^1u_k-\tilde{u}_k\|,$$

for $k=1,2,\dots,\ell$. Making use of B-spline functions, we write the interpolant $I_2^1u_k$ as

$$I_2^1u_k(x)=\sum_{j=0}^{N_x+1}\beta_{j,k}\mathfrak{B}_j(x),\quad\text{for } k=1,2,\dots,\ell.$$

$$[\boldsymbol{L}(\boldsymbol{\alpha}_k - \boldsymbol{\beta}_k)]_{j-1/2} = L_k(\tilde{u}_k - I_2^1 u_k)_{j-1/2} = \varepsilon^2 (I_2^1 u_k - u_k)_{j-1/2},\ j = 1, 2, \ldots, N_x.$$

Finally, Theorems 4.2 and 4.3 give

$$\|\boldsymbol{\alpha}_k - \boldsymbol{\beta}_k\| \leqslant C N_x^{-2}.$$

Since each $\mathfrak{B}_j \geqslant 0$ and the sum of all basis functions equals 1, so

$$\|I_2^1 \boldsymbol{u} - \tilde{\boldsymbol{u}}\| \leqslant \|\boldsymbol{\alpha}_k - \boldsymbol{\beta}_k\| \leqslant C N_x^{-2}.$$

We now apply Theorem 4.2 to complete the proof. □

5. Numerical outcomes and Discussion

In this section, we examine the verification of the theoretical estimates provided in the previous section by considering two numerical examples. The error estimates (in the maximum norm) are obtained by utilizing the double mesh principle [11]. The maximum pointwise error is computed as

$$e_{k,\varepsilon}^{N_x} = \max_j |\tilde{u}_k(x_{2j-1}) - \hat{u}_k(x_{j-1/2})|,$$

where $\hat{u}_k$ and $\tilde{u}_k$ represent the computed solutions by considering N_x and $2N_x$ mesh partitions, respectively. We also compute the corresponding order of convergence as

$$\eta_{k,\varepsilon}^{N_x} = \frac{\ln(e_{k,\varepsilon}^{N_x} / e_{k,\varepsilon}^{2N_x})}{\ln 2}.$$

Furthermore, we calculate the ε-uniform maximum pointwise error $e_k^{N_x}$ and the corresponding ε-uniform order of convergence $\eta_k^{N_x}$ as follows

$$e_k^{N_x} = \max_\varepsilon e_{k,\varepsilon}^{N_x},$$
$$\eta_k^{N_x} = \frac{\ln(e_k^{N_x} / e_k^{2N_x})}{\ln 2}.$$

Remark 5.1. All the above estimates are calculated for $k = 1, 2, \ldots, \ell$.

We have also calculated the overall error $\boldsymbol{e}^{N_x}$ as follows:

$$\boldsymbol{e}^{N_x} = \max_k (\max_\varepsilon e_{k,\varepsilon}^{N_x}).$$

Finally, the corresponding orders of convergence are given by

$$\boldsymbol{\eta}^{N_x} = \frac{\ln(\boldsymbol{e}^{N_x} / \boldsymbol{e}^{2N_x})}{\ln 2}.$$

From a practical point of view, we have calculated the uniform errors over a finite range of ε values ($\varepsilon = 1, 10^{-1}, \ldots, 10^{-10}$).

In the test problems, for simplicity, we take $\ell = 2$ in the first problem and $\ell = 3$ in the second problem. The solution components are denoted as u_k (exact solution) and $\tilde{u}_k$ (numerical solution), respectively. Moreover, the solution in vector form is denoted by bold letters.

Example 5.1. In this example, we consider the following system of 2 equations:

$$
\begin{aligned}
&-\varepsilon^2 u_1'' + 2(1+x)^2 u_1 - (1+x^3)u_2 = 2e^x,\\
&-\varepsilon^2 u_2'' - 2\cos\left(\frac{\pi x}{4}\right)u_1 + (1+\sqrt{2})e^{1-x}u_2 = 10x+1,\\
&u_1(0) = u_1(1) = 0, \quad u_2(0) = u_2(1) = 0.
\end{aligned}
$$

For this example, the matrix $\boldsymbol{B}$, $\boldsymbol{g}(x)$, $\boldsymbol{\varrho}_0$, and $\boldsymbol{\varrho}_1$ are as given below

$$
\boldsymbol{B} = \begin{bmatrix} 2(1+x)^2 & -(1+x^3) \\ -2\cos\left(\frac{\pi x}{4}\right) & (1+\sqrt{2})e^{1-x} \end{bmatrix}, \ \boldsymbol{g}(x) = (2e^x, 10x+1)^T,
$$
$$
\boldsymbol{\varrho}_0 = (0,0)^T, \ \boldsymbol{\varrho}_1 = (0,0)^T.
$$

Example 5.2. In this example, we consider the following system of 3 equations:

$$
\begin{aligned}
&-\varepsilon^2 u_1'' + 3u_1 + (1-x)(u_2 - u_3) = e^x,\\
&-\varepsilon^2 u_2'' + 2u_1 + (4+x)u_2 - u_3 = \cos x,\\
&-\varepsilon^2 u_3'' + 2u_1 + 3u_3 = 1 + x^2,\\
&u_1(0) = u_1(1) = 0, \quad u_2(0) = u_2(1) = 0, \quad u_3(0) = u_3(1) = 0.
\end{aligned}
$$

For this example, the matrix $\boldsymbol{B}$, $\boldsymbol{g}(x)$, $\boldsymbol{\varrho}_0$, and $\boldsymbol{\varrho}_1$ are as given below

$$
\boldsymbol{B} = \begin{bmatrix} 3 & 1-x & -(1-x) \\ 2 & 4+x & -1 \\ 2 & 0 & 3 \end{bmatrix}, \ \boldsymbol{g}(x) = (e^x, \cos x, 1+x^2)^T,
$$
$$
\boldsymbol{\varrho}_0 = (0,0,0)^T, \ \boldsymbol{\varrho}_1 = (0,0,0)^T.
$$

Table 1. Maximum pointwise errors $e_{1,\varepsilon}^{N_x}$ in the solution $\tilde{u}_1$ for Example 5.1

	N_x						
ε	64	128	256	512	1024	2048	4096
10^{-2}	$3.4414e-03$	$8.7439e-04$	$2.1556e-04$	$5.2958e-05$	$1.3095e-05$	$3.2550e-06$	$8.1124e-07$
	1.9766	2.0202	2.0252	2.0158	2.0083	2.0045	
10^{-4}	$3.4571e-03$	$8.7821e-04$	$2.1656e-04$	$5.3212e-05$	$1.3159e-05$	$3.2708e-06$	$8.1520e-07$
	1.9769	2.0198	2.0249	2.0157	2.0083	2.0045	
10^{-6}	$3.4573e-03$	$8.7825e-04$	$2.1658e-04$	$5.3215e-05$	$1.3159e-05$	$3.2710e-06$	$8.1529e-07$
	1.9769	2.0198	2.0249	2.0158	2.0083	2.0045	
10^{-8}	$3.4573e-03$	$8.7826e-04$	$2.1658e-04$	$5.3215e-05$	$1.3159e-05$	$3.2760e-06$	$8.2269e-07$
	1.9769	2.0198	2.0249	2.0158	2.0083	2.0045	
10^{-10}	$3.4573e-03$	$8.7826e-04$	$2.1658e-04$	$5.3215e-05$	$1.3159e-05$	$3.2765e-06$	$8.2278e-07$
	1.9769	2.0198	2.0249	2.0158	2.0083	2.0045	
$e_1^{N_x}$	$3.4573e-03$	$8.7826e-04$	$2.1658e-04$	$5.3215e-05$	$1.3159e-05$	$3.2765e-06$	$8.2278e-07$
$\eta_1^{N_x}$	1.9769	2.0202	2.0252	2.0158	2.0083	2.0045	
$C_1^{N_x}$	14.16	14.38	14.19	13.95	13.79	13.74	13.75

The solution of the system exhibits twin boundary layers in the neighborhoods of $x = 0$ and $x = 1$. As explained above, the uniform mesh is unsuitable for resolving

Table 2. Maximum pointwise errors $e_{2,\varepsilon}^{N_x}$ in the solution $\tilde{u}_2$ for Example 5.1

ε	N_x 64	128	256	512	1024	2048	4096
10^{-2}	$7.0349e-03$	$1.7946e-03$	$4.4247e-04$	$1.0926e-04$	$2.7095e-05$	$6.7447e-06$	$1.6824e-06$
	1.9709	2.0200	2.0178	2.0117	2.0062	2.0032	
10^{-4}	$7.1101e-03$	$1.8146e-03$	$4.4739e-04$	$1.1048e-04$	$2.7400e-05$	$6.8205e-06$	$1.7013e-06$
	1.9702	2.0200	2.0177	2.0115	2.0062	2.0032	
10^{-6}	$7.1109e-03$	$1.8148e-03$	$4.4744e-04$	$1.1049e-04$	$2.7403e-05$	$6.8213e-06$	$1.7016e-06$
	1.9702	2.0200	2.0177	2.0115	2.0062	2.0032	
10^{-8}	$7.1109e-03$	$1.8148e-03$	$4.4746e-04$	$1.1048e-04$	$2.7411e-05$	$6.8213e-06$	$1.7160e-06$
	1.9702	2.0200	2.0177	2.0115	2.0062	2.0032	
10^{-10}	$7.1109e-03$	$1.8148e-03$	$4.4746e-04$	$1.1048e-04$	$2.7414e-05$	$6.8220e-06$	$1.7169e-06$
	1.9702	2.0200	2.0177	2.0115	2.0062	2.0032	
$e_2^{N_x}$	$7.1109e-03$	$1.8148e-03$	$4.4746e-04$	$1.1048e-05$	$2.7414e-05$	$6.8220e-06$	$1.7169e-06$
$\eta_2^{N_x}$	1.9702	2.0200	2.0178	2.0117	2.0062	2.0032	
$C_2^{N_x}$	29.12	29.73	29.32	28.96	28.74	28.61	28.60

these layers, and one cannot obtain parameter-uniform estimates on this mesh. So, the numerical results for both examples are obtained using the exponentially graded mesh (eXp mesh). Tables 1 and 2 show the parameter-uniform results for the solutions $\tilde{u}_1$ and $\tilde{u}_2$ in Example 5.1, which are second-order uniformly convergent. Similarly, for Example 5.2, we obtain the parameter-uniform estimates of order $O(N_x^{-2})$ for $\tilde{u}_1$, $\tilde{u}_2$, and $\tilde{u}_3$, respectively (refer to Tables 3, 4, and 5). We have also computed the results for the Shishkin mesh and Bakhvalov-Shishkin (B-S) mesh and compared the results on these meshes in Tables 6 and 7. This comparison suggests a parameter-uniform convergence of orders $O(N_x^{-2})$, $O(N_x^{-2}\ln^2 N_x)$, and $O(N_x^{-2})$, respectively. To support this, we have also calculated ε-uniform orders of convergence and ε-uniform error constants (see [13] for the computation of C^{N_x}).

Furthermore, we combine the mesh plots of the considered meshes (eXp, Shishkin, and B-S) in a single plot that shows the distribution of mesh points in the layer regions and regular regions. Since the eXp and the B-S mesh differ by a slight change in the choice of the mesh generating function $\Psi(\rho)$, the mesh points coincide in the plot. We have displayed the presence of boundary layers in the solution by plotting the 2-D graphs. From Fig. 2 it is observed that the boundary layers for $\varepsilon = 10^{-4}$ are stiffer (see Figs. 2(b) and 2(d)) as compared to the boundary layers for $\varepsilon = 10^{-2}$ (see Figs. 2(a) and 2(c)) which confirms the theory that for SPBVPs the width of the boundary layer decreases as ε decreases.

Remark 5.2. In Fig. 2, $u_{\Delta;k}$ represents the k^{th} component of the numerical solution on the partition Δ.

6. Concluding Remarks

A numerical scheme that uses the quadratic B-spline functions on an exponentially graded mesh has been developed for a weakly coupled system of ℓ singularly perturbed reaction-diffusion equations. The main reason to choose the exponentially graded mesh is its advantage over other meshes like Shishkin and Bakhvalov-type meshes, as it does not require prior information about the transition parameter *i.e.,* it is independent of the transition point(s). The estimated theoretical bounds

Table 3. Maximum pointwise errors $e_{1,\varepsilon}^{N_x}$ in the solution $\tilde{u}_1$ for Example 5.2

	N_x						
ε	64	128	256	512	1024	2048	4096
10^{-2}	$1.8695e-03$	$4.7469e-04$	$1.1770e-04$	$2.9012e-05$	$7.1840e-06$	$1.7866e-06$	$4.4546e-07$
	1.9776	2.0119	2.0204	2.0138	2.0076	2.0038	
10^{-4}	$1.8675e-03$	$4.7416e-04$	$1.1756e-04$	$2.8978e-05$	$7.1757e-06$	$1.7845e-06$	$4.4494e-07$
	1.9777	2.0120	2.0204	2.0138	2.0076	2.0038	
10^{-6}	$1.8675e-03$	$4.7416e-04$	$1.1756e-04$	$2.8978e-05$	$7.1757e-06$	$1.7845e-06$	$4.4496e-07$
	1.9776	2.0120	2.0204	2.0138	2.0076	2.0038	
10^{-8}	$1.8675e-03$	$4.7416e-04$	$1.1756e-04$	$2.8978e-05$	$7.1757e-06$	$1.7845e-06$	$4.4496e-07$
	1.9776	2.0120	2.0204	2.0138	2.0076	2.0038	
10^{-10}	$1.8675e-03$	$4.7416e-04$	$1.1756e-04$	$2.8978e-05$	$7.1757e-06$	$1.7845e-06$	$4.4496e-07$
	1.9776	2.0120	2.0204	2.0138	2.0076	2.0038	
$e_1^{N_x}$	$1.8675e-03$	$4.7469e-04$	$1.1770e-04$	$2.9012e-05$	$7.1840e-06$	$1.7845e-06$	$4.4496e-06$
$\eta_1^{N_x}$	1.9776	2.0120	2.0204	2.0138	2.0076	2.0038	
$C_1^{N_x}$	7.64	7.76	7.70	7.59	7.52	7.48	7.49

Table 4. Maximum pointwise errors $e_{2,\varepsilon}^{N_x}$ in the solution $\tilde{u}_2$ for Example 5.2

	N_x						
ε	64	128	256	512	1024	2048	4096
10^{-2}	$7.2661e-04$	$1.9713e-04$	$4.8933e-05$	$1.2064e-05$	$2.9843e-06$	$7.4152e-07$	$1.8478e-07$
	1.8820	2.0103	2.0201	2.0152	2.0088	2.0047	
10^{-4}	$7.2739e-04$	$1.9735e-04$	$4.8989e-05$	$1.2078e-05$	$2.9877e-06$	$7.4238e-07$	$1.8500e-07$
	1.8820	2.0102	2.0201	2.0153	2.0088	2.0046	
10^{-6}	$7.2740e-04$	$1.9735e-04$	$4.8989e-05$	$1.2078e-05$	$2.9878e-06$	$7.4239e-07$	$1.8500e-07$
	1.8820	2.0102	2.0201	2.0153	2.0088	2.0046	
10^{-8}	$7.2740e-04$	$1.9735e-04$	$4.8989e-05$	$1.2078e-05$	$2.9878e-06$	$7.4239e-07$	$1.8500e-07$
	1.8820	2.0102	2.0201	2.0153	2.0088	2.0046	
10^{-10}	$7.2740e-04$	$1.9735e-04$	$4.8989e-05$	$1.2078e-05$	$2.9878e-06$	$7.4239e-07$	$1.8500e-07$
	1.8820	2.0102	2.0201	2.0153	2.0088	2.0046	
$e_2^{N_x}$	$7.2740e-04$	$1.9735e-04$	$4.8989e-05$	$1.2078e-05$	$2.9878e-06$	$7.4239e-07$	$1.8500e-07$
$\eta_2^{N_x}$	1.9702	2.0200	2.0178	2.0117	2.0062	2.0032	
$C_2^{N_x}$	2.97	3.23	3.21	3.16	3.13	3.11	3.10

Table 5. Maximum pointwise errors $e_{3,\varepsilon}^{N_x}$ in the solution $\tilde{u}_3$ for Example 5.2

	N_x						
ε	64	128	256	512	1024	2048	4096
10^{-2}	$1.4829e-03$	$4.1205e-04$	$1.0335e-04$	$2.5429e-05$	$6.2959e-06$	$1.5641e-06$	$3.8974e-07$
	1.8475	1.9953	2.0230	2.0140	2.0091	2.0047	
10^{-4}	$1.4837e-03$	$4.1227e-04$	$1.0340e-04$	$2.5442e-05$	$6.2991e-06$	$1.5648e-06$	$3.8993e-07$
	1.8475	1.9954	2.0230	2.0140	2.0091	2.0047	
10^{-6}	$1.4838e-03$	$4.1227e-04$	$1.0340e-04$	$2.5442e-05$	$6.2991e-06$	$1.5648e-06$	$3.8993e-07$
	1.8475	1.9954	2.0230	2.0140	2.0091	2.0047	
10^{-8}	$1.4837e-03$	$4.1227e-04$	$1.0340e-04$	$2.5442e-05$	$6.2991e-06$	$1.5648e-06$	$3.8993e-07$
	1.8475	1.9954	2.0230	2.0140	2.0091	2.0047	
10^{-10}	$1.4837e-03$	$4.1227e-04$	$1.0340e-04$	$2.5442e-05$	$6.2991e-06$	$1.5648e-06$	$3.8993e-07$
	1.8475	1.9954	2.0230	2.0140	2.0091	2.0047	
$e_3^{N_x}$	$1.4837e-03$	$4.1227e-03$	$1.0340e-04$	$2.5442e-05$	$6.2991e-06$	$1.5648e-06$	$3.8993e-07$
$\eta_3^{N_x}$	1.8475	1.9954	2.0230	2.0140	2.0091	2.0047	
$C_3^{N_x}$	6.07	6.75	6.77	6.66	6.60	6.56	6.55

Table 6. Uniform maximum pointwise errors comparison in the solution for Example 5.1

	eXp mesh			Shishkin mesh			B-S mesh		
N_x	$\boldsymbol{e}^{N_x}$	$\boldsymbol{\eta}^{N_x}$	C^{N_x}	$\boldsymbol{e}^{N_x}$	$\boldsymbol{\eta}^{N_x}$	C^{N_x}	$\boldsymbol{e}^{N_x}$	$\boldsymbol{\eta}^{N_x}$	C^{N_x}
128	1.814(−3)	2.019	29.73	6.114(−3)	1.622	16.41	1.784(−3)	2.006	29.23
256	4.474(−4)	2.018	29.32	1.986(−3)	1.672	16.42	4.440(−4)	2.013	29.10
512	1.104(−4)	2.010	28.96	6.232(−4)	1.706	15.86	1.100(−4)	2.008	28.84
1024	2.741(−5)	2.006	28.74	1.910(−4)	1.774	14.97	2.734(−5)	2.001	28.67
2048	6.821(−6)	1.990	28.61	5.584(−5)	1.921	13.47	6.828(−6)	1.994	28.64
4096	1.716(−6)	-	28.60	1.474(−5)	-	10.95	1.714(−7)	-	28.61

Table 7. Uniform maximum pointwise errors comparison in the solution for Example 5.2

	eXp mesh			Shishkin mesh			B-S mesh		
N_x	$\boldsymbol{e}^{N_x}$	$\boldsymbol{\eta}^{N_x}$	C^{N_x}	$\boldsymbol{e}^{N_x}$	$\boldsymbol{\eta}^{N_x}$	C^{N_x}	$\boldsymbol{e}^{N_x}$	$\boldsymbol{\eta}^{N_x}$	C^{N_x}
128	4.741(−4)	2.012	7.76	1.442(−3)	1.563	2.92	4.672(−4)	2.002	7.65
256	1.175(−4)	2.020	7.70	4.878(−4)	1.672	2.92	1.166(−4)	2.014	7.64
512	2.897(−5)	2.013	7.59	1.530(−4)	1.707	2.71	2.886(−5)	2.010	7.56
1024	7.175(−6)	2.007	7.52	4.685(−5)	1.768	2.45	7.161(−6)	2.004	7.50
2048	1.784(−6)	2.003	7.48	1.375(−5)	1.891	2.12	1.785(−6)	1.994	7.48
4096	4.449(−7)	-	7.49	3.706(−6)	-	1.70	4.446(−7)	-	7.49

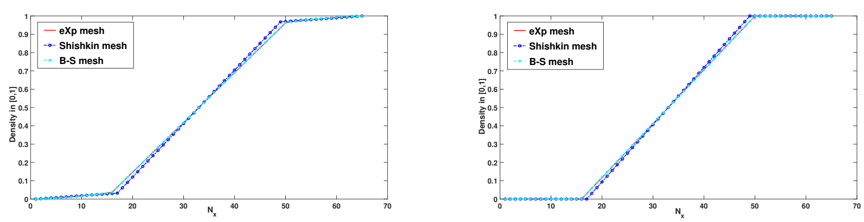

(a) $\varepsilon = 2^{-8}$ (b) $\varepsilon = 2^{-20}$

Figure 1. Mesh comparison of eXp mesh, Shishkin mesh, B-S mesh for $N_x = 64$

on the spline interpolation error show that the method is second-order convergent irrespective of the value of $\mathcal{E}$. The numerical results in the tables validate the theoretical estimates regarding the orders of convergence and the errors estimated in Section 4.

Acknowledgement. The authors are grateful to the unknown reviewers for their insightful observations leading to the improvement of the manuscript.

Declarations.

Ethical Approval and Consent to participate. The consent is taken from all the authors, and all authors approve the submission of the manuscript.

Competing interests. The authors state that they have no known competing interests.

Authors' contributions. Satpal Singh- Writing, editing, conceptualization. Devendra Kumar- Writing, editing, review, supervision. Higinio Ramos- editing, review.

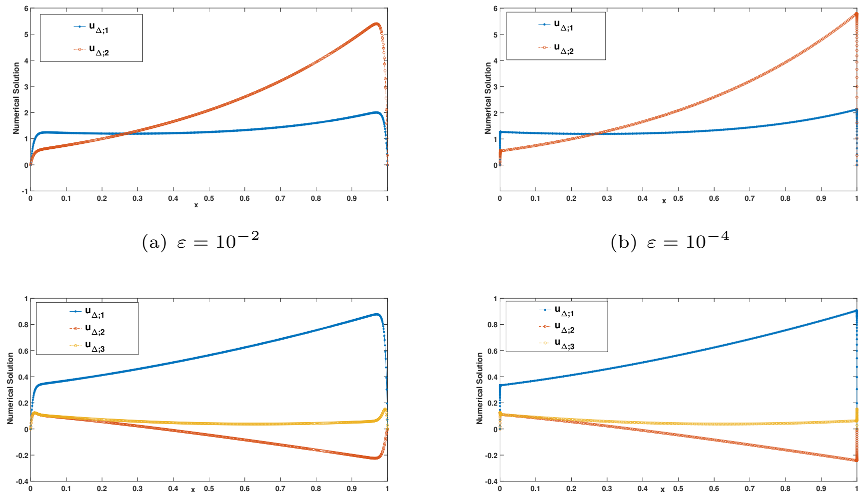

(a) $\varepsilon = 10^{-2}$ (b) $\varepsilon = 10^{-4}$

(c) $\varepsilon = 10^{-2}$ (d) $\varepsilon = 10^{-4}$

Figure 2. Numerical solution plots of Example 5.1 (subfigures (a) and (b)), and Example 5.2 (subfigures (c) and (d))

References

[1] M. P. Alam, D. Kumar and A. Khan, *Trigonometric quintic B-spline collocation method for singularly perturbed turning point boundary value problems*, Int. J. Comput. Math., 2021, 98(5), 1029–1048.

[2] N. S. Bakhvalov, *Towards optimization of methods for solving boundary value problems in the presence of boundary layers*, Zh. Vychisl. Mat. Mat. Fiz., 1969, 9(4), 841–859.

[3] G. I. Barenblatt, I. P. Zheltov and I. N. Kochina, *Basic concepts in the theory of seepage of homogeneous liquids in fissured rocks*, J. Appl. Math. Mech., 1960, 24(5), 1286–1303.

[4] C. De Boor and B. Swartz, *Collocation at Gaussian points*, SIAM J. Numer. Anal., 1973, 10(4), 582–606.

[5] C. Clavero, J. L. Gracia and F. J. Lisbona, *High order schemes for reaction-diffusion singularly perturbed systems*, Lect. Notes Comput. Sci. Eng., 2009, 69, 107–115.

[6] C. Clavero, J. L. Gracia and F. J. Lisbona, *An almost third order finite difference scheme for singularly perturbed reaction-diffusion systems*, J. Comput. Appl. Math., 2010, 234(8), 2501–2515.

[7] P. Constantinou and C. Xenophontos, *Finite element analysis of an exponentially graded mesh for singularly perturbed problems*, Comput. Methods Appl. Math., 2015, 15(2), 135–143.

[8] S. C. Cowin, *Bone poroelasiticity*, J. Biomech., 1999, 32(3), 217–238.

[9] P. Das and S. Natesan, *Optimal error estimate using mesh equidistribution*

technique for singularly perturbed system of reaction-diffusion boundary-value problems, Appl. Math. Comput., 2014, 249, 265–277.

[10] P. Das and J. Vigo-Aguiar, *Parameter uniform optimal order numerical approximation of a class of singularly perturbed system of reaction diffusion problems involving a small perturbation parameter*, J. Comput. Appl. Math., 2019, 354, 533–544.

[11] E. P. Doolan, J. J. H. Miller and W. H. A. Schilders, *Uniform Numerical Methods for Problems with Initial and Boundary Layers*, Boole Press, Dublin, 1980.

[12] P. A. Farrell, P. W. Hemker and G. I. Shishkin, *Discrete approximations for singularly perturbed boundary value problems with parabolic layers*, J. Comput. Math., 1996, 14(1), 71–97.

[13] P. A. Farrell, A. F. Hegarty, J. J. H. Miller, E. O'Riordan and G. I. Shishkin, *Robust Computational Techniques for Boundary Layers*, Chapman & Hall/CRC, Boca Raton, FL, 2000.

[14] W. J. Kammerer, G. W. Reddien and R. S. Varga, *Quadratic interpolatory splines*, Numer. Math., 1974, 22, 241–259.

[15] Y. Kan-On and M. Mimura, *Singular perturbation approach to a 3-component reaction-diffusion system arising in population dynamics*, SIAM J. Math. Anal., 1998, 29(6), 1519–1536.

[16] R. B. Kellogg, N. Madden and M. Stynes, *A parameter-robust numerical method for a system of reaction-diffusion equations in two dimensions*, Numer. Methods Partial Differential Equations, 2008, 24, 312–334.

[17] R. B. Kellogg, T. Linßand M. Stynes, *A finite difference method on layer-adapted meshes for an elliptic reaction-diffusion system in two dimensions*, Math. Comp., 2008, 77(264), 2085–2096.

[18] N. Kopteva, *Maximum norm a posteriori error estimates for a 1D singularly perturbed semilinear reaction diffusion problem*, IMA J. Numer. Anal., 2007, 27(3), 576–592.

[19] D. Kumar, *A parameter-uniform scheme for the parabolic singularly perturbed problem with a delay in time*, Numer. Methods Partial Differential Equations, 2021, 37(1), 626–642.

[20] D. Kumar and P. Kumari, *Uniformly convergent scheme for two-parameter singularly perturbed problems with non-smooth data*, Numer. Methods Partial Differential Equations, 2021, 37(1), 796–817.

[21] O. A. Ladyzhenskaya and N. N., Ural'tseva, *Linear and quasilinear elliptic equations*, Leon Ehrenpreis Academic Press, New York, 1968.

[22] R. Lin and M. Stynes, *A balanced finite element method for a system of singularly perturbed reaction-diffusion two-point boundary value problems*, Numer. Algorithms, 2015, 70, 691–707.

[23] T. Linß, *An upwind difference scheme on a novel Shishkin-type mesh for a linear convection-diffusion problem*, J. Comput. Appl. Math., 1999, 110(1), 93–104.

[24] T. Linß, *Analysis of a Galerkin finite element Shishkin mesh for a linear convection-diffusion method on a Bakhvalov-problem*, IMA J. Numer. Anal., 2000, 20(4), 621–632.

[25] T. Linßand N. Madden, *Accurate solution of a system of coupled singularly perturbed reaction-diffusion equations*, Computing, 2004, 73, 121–133.

[26] T. Linßand N. Madden, *A finite element analysis of a coupled system of singularly perturbed reaction-diffusion equations*, Appl. Math. Comput., 2004, 148(3), 869–880.

[27] T. Linß, *Layer-adapted meshes for one-dimensional reaction-convection-diffusion problems*, J. Numer. Math., 2004, 12(3), 193–205.

[28] T. Linßand N. Madden, *Layer-adapted meshes for a linear system of coupled singularly perturbed reaction-diffusion problems*, IMA J. Numer. Anal., 2009, 29(1), 109–125.

[29] T. Linß, *Analysis of a FEM for a coupled system of singularly perturbed reaction-diffusion equations*, Numer. Algorithms, 2009, 50, 283–291.

[30] T. Linß, G. Radojev and H. Zarin, *Approximation of singularly perturbed reaction-diffusion problems by quadratic C^1-splines*, Numer. Algorithms, 2012, 61, 35–55.

[31] N. Madden, *Numerical methods for wave-current interactions*, Ph.D., National University of Ireland, Cork, 2000.

[32] N. Madden and M. Stynes, *A uniformly convergent numerical method for a coupled system of singularly perturbed linear reaction-diffusion problems*, IMA J. Numer. Anal., 2003, 23(4), 627–644.

[33] M. J. Marsden, *Quadratic spline interpolation*, Bull. Amer. Math. Soc., 1974, 80(5), 903–906.

[34] S. Matthews, *Parameter robust methods for a system of coupled singularly perturbed ordinary differential reaction-diffusion equations*, M.Sc., School of Mathematical Sciences, Dublin City University, 2000.

[35] S. Matthews, J. J. H. Miller, E. O'Riordan and G. I. Shishkin, *Parameter-robust numerical methods for a system of reaction-diffusion problems with boundary layers*, in: J.J.H. Miller, G.I. Shishkin, L. Vulkov (Eds.), *Analytical and Numerical Methods for Convection-Dominated and Singularly Perturbed Problems*, Nova Science Publishers, Inc., New York, USA, 2000, 219–224.

[36] S. Matthews, E. O'Riordan and G. I. Shishkin, *A numerical method for a system of singularly perturbed reaction-diffusion equations*, J. Comput. Appl. Math., 2002, 145(1), 151–166.

[37] J. J. H. Miller, E. O'Riordan and G. I. Shishkin, *On piecewise-uniform meshes for upwind and central-difference operators for solving singularly perturbed problems*, IMA J. Numer. Anal., 1995, 15(1), 89–99.

[38] J. J. H. Miller, E. O'Riordan and G. I. Shishkin, *Fitted Numerical Methods for Singular Perturbation Problems*, World Scientific, Singapore, 1996.

[39] D. S. Naidu and A. J. Calise, *Singular perturbations and time scales in guidance and control of aerospace systems: a survey*, J. Guid. Control Dyn., 2001, 24(6), 1057–1078.

[40] S. Natesan and B. S. Deb, *A Robust computational method for singularly perturbed coupled system of reaction-diffusion boundary-value problems*, Appl. Math. Comput., 2007, 188(1), 353–364.

[41] T. A. Nhan and R. Vulanović, *The Bakhvalov mesh: a complete finite-difference analysis of two-dimensional singularly perturbed convection-diffusion problems*, Numer. Algorithms, 2021, 87, 203–221.

[42] M. H. Protterand H. F. Weinberger, *On the spectrum of general second-order operators*, Bull. Amer. Math. Soc., 1966, 72, 251–255.

[43] E. O'Riordan and M. Stynes, *A uniformly accurate finite-element method for a singularly perturbed one-dimensional reaction-diffusion problem*, Math. Comp., 1986, 47(176), 555–570.

[44] W. Rodi, *Turbulence Models and Their Applications in Hydraulics (A. A. Balkema, ed.)*, IAHR Monograph Series, Rotterdam, 3rd edition, 1993.

[45] H. G. Roos, M. Stynes and L. Tobiska, *Numerical Methods for Singularly Perturbed Differential Equations, Convection-Diffusion and Flow Problems*, Springer-Verlag, New York, 1996.

[46] W. Ruan and C. Pao, *Asymptotic behavior and positive solutions of a chemical reaction diffusion system*, J. Math. Anal. Appl., 1992, 169(1), 157–178.

[47] G. I. Shishkin, *Mesh approximation of singularly perturbed boundary-value problems for systems of elliptic and parabolic equations*, Comput. Maths. Math. Phys., 1995, 4(35), 429–446.

[48] M. Shivhare, P. C. Podila and D. Kumar, *A uniformly convergent quadratic B-spline collocation method for singularly perturbed parabolic partial differential equations with two small parameters*, J. Math. Chem., 2021, 59, 186–215.

[49] G. Singh and S. Natesan, *A uniformly convergent numerical scheme for a coupled system of singularly perturbed reaction-diffusion equations*, Numer. Funct. Anal. Opti., 2020, 41(10), 1172–1189.

[50] S. Singh, D. Kumar and H. Ramos, *A uniformly convergent quadratic B-spline based scheme for singularly perturbed degenerate parabolic problems*, Math. Comput. Simulation, 2022, 195, 88–106.

[51] M. Stephens and N. Madden, *A parameter-uniform Schwarz method for a coupled system of reaction-diffusion equations*, J. Comput. Appl. Math., 2009, 230(2), 360–370.

[52] G. P. Thomas, *Towards an improved turbulence model for wave-current interactions,* in: Second Annual Report to EU MAST-III Project "The Kinematics and Dynamics of Wave-Current Interactions", 1998.

[53] T. Valanarasu and N. Ramanujam, *An asymptotic initial value method for boundary value problems for a system of singularly perturbed second order ordinary differential equations*, Appl., Math. Comput., 2004, 147(1), 227–240.

[54] R. Vulanović, *Non-equidistant generalizations of the Gushchin-Schennikov scheme*, ZAAM-J. Appl. Math. Mech., 1987, 67(12), 625–632.

[55] H. Zarin, *Exponentially graded mesh for singularly perturbed problem with two small parameters*, Appl. Numer. Math., 2017, 120, 233–242.